

See discussions, stats, and author profiles for this publication at: <https://www.researchgate.net/publication/231627195>

Dynamic Responses of a Thermotropic Main-Chain Liquid Crystalline Polyester during Polymerization under Electric Fields

ARTICLE *in* THE JOURNAL OF PHYSICAL CHEMISTRY B · OCTOBER 2000

Impact Factor: 3.3 · DOI: 10.1021/jp000518p

CITATION

1

READS

13

2 AUTHORS:



Si-Xue Cheng

Wuhan University

186 PUBLICATIONS 5,143 CITATIONS

SEE PROFILE



Tai-Shung Chung

National University of Singapore

726 PUBLICATIONS 19,531 CITATIONS

SEE PROFILE

Dynamic Responses of a Thermotropic Main-Chain Liquid Crystalline Polyester during Polymerization under Electric Fields

Si-Xue Cheng^{†,‡} and Tai-Shung Chung^{*,†,‡}

*Institute of Materials Research and Engineering, 3 Research Link, Singapore 117602, and
Department of Chemical and Environmental Engineering, National University of Singapore,
10 Kent Ridge Crescent, Singapore 119260*

Received: February 9, 2000; In Final Form: August 8, 2000

The dynamic responses of a main-chain liquid crystalline polymer (LCP) during the polycondensation reaction under electric fields have been studied for the first time by a modified thin-film polymerization technique using a polarizing microscope. The evolution of the in situ liquid crystal (LC) texture during polymerization under electric fields is found to be quite different from that without electric fields. Compared to the low-molecular-weight LC systems, the polymerized thermotropic poly(*p*-oxybenzoate/2,6-oxy-naphthoate) (P(OBA/ONA)) system does not show distinct morphological change from the fluctuating Williams domains to the dynamic scattering mode. The dynamic response of the LC phase during the polymerization is strongly dependent on the frequency and strength of the external field. In a low-frequency range, molecular orientation is found to be in the low-voltage range. In a medium-frequency range, electric field induced flow (electrohydrodynamic instability) is observed. In a high-frequency range, LC molecular directors cannot respond fast enough, so the system appears to be stationary in a relatively wide voltage range. The changes in inherent properties of the reaction system also greatly affect the response of the LC phase to the electric field; thus, the electrohydrodynamic instability changes with the reaction time accordingly. The low- and high-frequency bounds of the electrohydrodynamic flow regime decrease with an increase in reaction time.

1. Introduction

Since the electro-optical effect of liquid crystals (LCs) was discovered and extensive applications were recognized, the effects of an electric field on liquid crystal materials have been of considerable interest to both academia and industry.^{1–14} The direct influences of the electric field on LC include a shift in the phase transition temperature, variation in order parameter, and a change in symmetry.²

Because of the dielectric anisotropy property of LCs, the LC molecules can theoretically align either parallel or perpendicular to the electric field according to their dielectric anisotropy values.¹ However, under certain conditions, the uniform director orientation under an ac electric field is energetically unfavorable; therefore, the domain structure corresponding to minimum free energy is formed. The domain patterns can be classified into two main types: the orientational domains with pure director rotation without fluid motion and the electrohydrodynamic domains caused by the combined effects of the periodic director reorientation and regular vortices of material motion.² This kind of vortical movement is called “hydrodynamic flow”, mainly a result of the effects of conductivity anisotropy of LC molecules and ionic electric current.

The movement of LC materials in an electric field is known as “electrohydrodynamic instability”.^{1–3} Theoretically it occurs when the dielectric anisotropy and the conductivity anisotropy have different signs, most commonly with negative dielectric anisotropy and positive conductivity anisotropy. The domain formation is also greatly dependent on the parameters of external

fields. In a low-frequency region, the most frequently observed domain is called the “Williams domain” or the “Kapustin–Williams domain”, caused by a periodic distortion accompanied by cellular flow. The spatial period is slightly shorter than the sample thickness. This frequency region is known as the “conduction regime”. In many cases, the Williams domain pattern is a simple one-dimensional pattern, and the pattern stays the same when the electric field reverses. However, the pattern may be interrupted, and a two-dimensional periodicity can be observed. The two-dimensional pattern has been identified as “fluctuating Williams domains”.^{11,12} In the high-frequency region, a narrow band mode called the “Chevron pattern” can be observed. This frequency region is called the “dielectric regime”, where the charge oscillations cause the oscillations of LC materials so that the vortices are not stationary but move “to and fro”.^{1,2}

Usually, there exists a threshold voltage of formation for the domain structure. The threshold value is determined by the physical properties of each LC, such as dielectric and conductivity anisotropies, viscoelastic properties, and experiment conditions like amplitude and frequency of the external field, cell thickness, and initial orientation. The previous work^{1,2} suggests that the threshold voltage of formation for the Williams domains is not strongly dependent on the frequency while the threshold voltage for the Chevron pattern increases with increasing frequency. With further increases in voltage, the flow velocity increases, and finally, above a certain voltage, a new regime is reached where the domain becomes disordered and mobile and the flow becomes turbulent. The latter phenomenon results in strong light scattering, known as “dynamic scattering”.^{1–3}

Although there is a fair amount of knowledge about liquid crystalline polymers (LCPs),^{15–19} the study of electrical re-

* Corresponding author. E-mail: chencts@nus.edu.sg. Fax: 65–7791936.

[†] Institute of Materials Research and Engineering.

[‡] National University of Singapore.

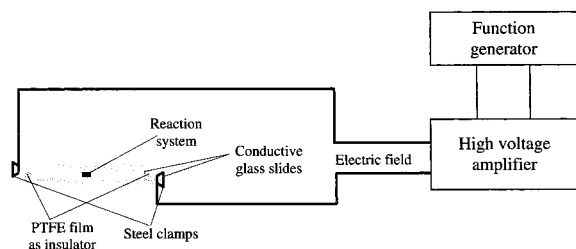


Figure 1. Thin-film polymerization under an ac electric field.

sponses of thermotropic main-chain liquid crystalline polymers (MCLCPs) under electrical fields is very limited. Most of the research was concentrated on low-molecular-weight liquid crystals (LMWLCs).^{4–10} Only a few papers reported the effects of electrical fields on thermotropic MCLCPs.^{11,12} In those studies, the Kapustin–Williams domains and light dynamic scattering^{11,12} were observed for the polymeric nematics. The observed electrohydrodynamic instability of LCPs was similar to that of LMWLCs. However, the major differences between them were the slow dynamics of the domain formation and the difficulty in obtaining a well-aligned pattern for LCPs.^{11,12} The

frequency to induce instability in the conduction regime was found to be strongly dependent on the molecular weight.¹¹

Another important issue for MCLCPs is that most monomers for LCP synthesis do not possess liquid crystallinity. However, the LC phase forms during polymerization, and the LC texture evolves with the progress of polymerization.¹⁹ To the best of our knowledge, the in situ LC texture evolution for MCLCPs during the polycondensation reaction under an electric field has not been reported by other researchers. Using a thin-film polymerization technique, our research group has examined in situ the morphological changes of polymerization systems by a polarizing microscope.^{20–24} In this paper, we intend to apply this technique, with proper modifications, to study the fundamentals of LCP polymerization under an electric field.

2. Experimental Section

2.1. Preparation of Monomers. *p*-Acetoxybenzoic acid (ABA) and 2,6-acetoxynaphthoic acid (ANA) were prepared by the acetylation of *p*-hydroxybenzoic acid (HBA) and 2,6-hydroxynaphthoic acid (HNA), respectively. The prepared ABA monomer was then purified by recrystallization in butyl acetate,

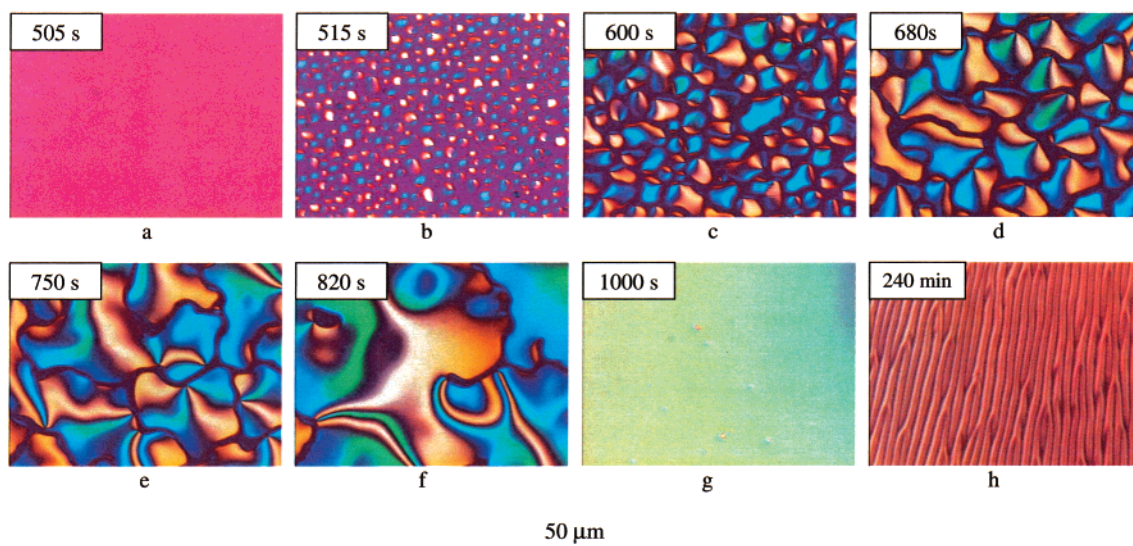


Figure 2. Micrographs showing morphological changes of the polymerization reaction system without an electric field. All micrographs were obtained from the same area of the same sample. Monomer composition: 73/27 ABA/ANA. Reaction temperature: 230 °C.

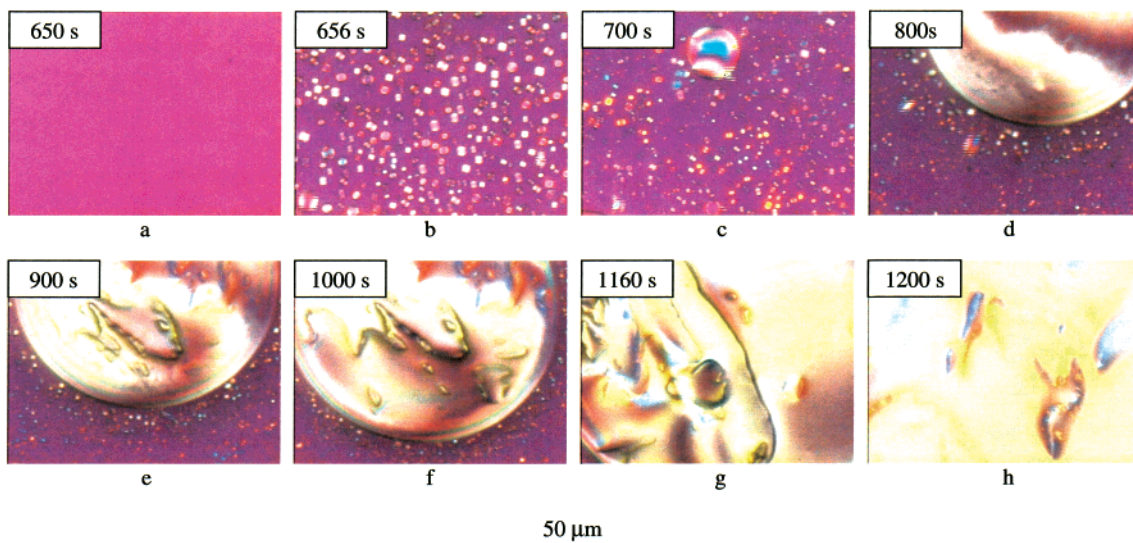


Figure 3. Appearances of the LC phase between two conductive glasses (without electric field). Monomer composition: 73/27 ABA/ANA. Reaction temperature: 230 °C.

whereas ANA was purified in methanol.²⁰ The melting points of ABA and ANA, measured with a DSC instrument (Perkin-Elmer DSC Pyris 1), are 196 and 226 °C, respectively. ¹H NMR was used to confirm the success of the acetylation for these monomers.

2.2. Thin-Film Polymerization. **2.2.1. Thin-Film Polymerization without an Electric Field.** The 73/27 (mole ratio) ABA/ANA composition was chosen for the study because this is the composition of commercially available Vectra A. The monomer mixture was placed on a glass slide, and a drop of acetone was deposited onto the glass slide to dissolve the mixture to form a thin reactant layer attached to the glass slide after acetone evaporation. It was then assembled like a sandwich, with a ring spacer between two glass slides, where the reactant layer was attached on the top slide. The ring spacer was made of stainless steel with a thickness of 0.5 mm. The whole package was placed on the heating stage (Linkam THMS-600) of a microscope and heated to a proposed temperature. The sample was held at the specific temperature during the entire reaction process. When the heating stage reached the proposed temperature, recording of the reaction time was begun. The temperature of the top slide was calibrated by the melting points of pure monomers as well as by a thermocouple. The polymerization reaction was carried out on the top slide, and all the temperatures reported here refer to the temperatures of the top slide. The thickness of the polycondensation reaction system was controlled at about 10 μm . The reaction process was observed in situ by a polarizing light microscope (Olympus BX50) with crossed polarizers. The optical images were recorded with the Image-Pro Plus software and a digital video cassette recorder (SONY DHR-1000NP).^{20–24}

2.2.2. Thin-Film Polymerization under Electric Fields. For the thin-film polymerization under electric fields, the sample package and connection of electric devices are shown in Figure 1. Following the approach illustrated in section 2.2.1, a thin layer of reactant mixture was formed. The reaction system was directly sandwiched between two conductive glass slides coated with indium tin oxide (ITO). On the edge of the glass slide, a poly(tetrafluoroethylene) (PTFE) film was used as a spacer as well as an insulator. The thickness of the reactant layer was increased to 80 μm so that the electrohydrodynamic instability could be clearly observed. The conductive glass slides were connected to the outputs of a high-voltage amplifier through the wires clamped by steel clamps. The electric field was generated by a functional generator (HP 33120A) and was amplified by a high-voltage amplifier (Trek P0623A). The electric fields (square wave) with different frequencies and voltages were applied to the reaction system after the generation of the LC phase. During the polymerization, the electric resistance of the reaction system was measured with a multimeter (Fluke 75).

2.3. FTIR Characterization. The monomer mixture and the polymer were characterized with a FTIR instrument (Perkin-Elmer FTIR Spectrometer Spectrum 2000). The polymer sample (in KBr pellet) was prepared by scraping the material from the glass slide after polymerization.

3. Results and Discussion

3.1. Morphology of the LCP Polymerization System without an Electric Field. To investigate the effect of electric fields on the polymerization of LCP, we compared polymerizations with and without electric fields. For the thin-film polymerization without electric fields, we have reported the results in detail in our previous papers.^{20–24} Here, we only briefly summarize the morphological changes. Figure 2 shows the

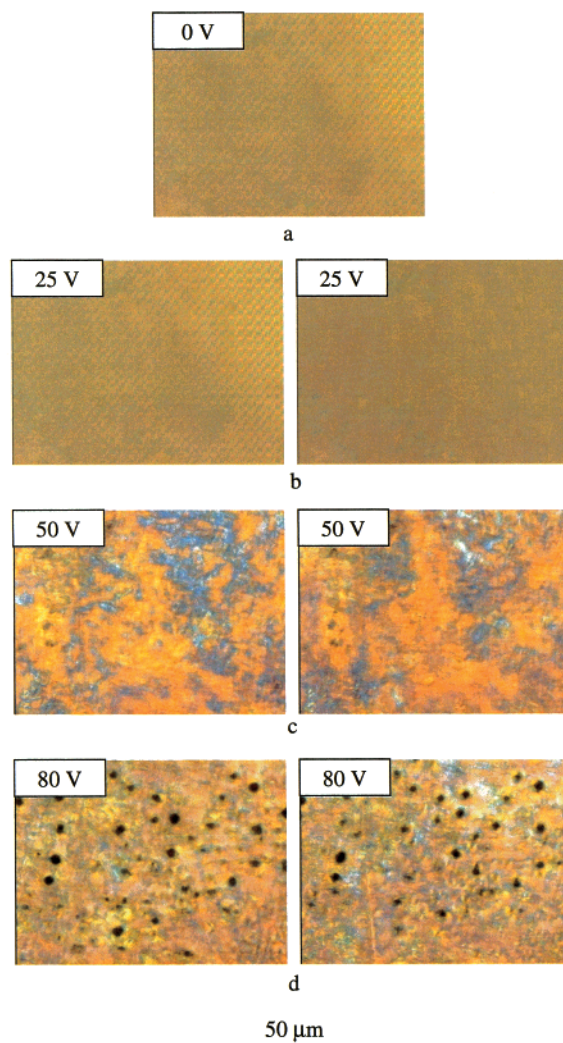


Figure 4. Morphologies of the LC phase under ac electric fields with 1 Hz frequency and different voltages: (a) 0, (b) 25, (c) 50, and (d) 80 V. Range of reaction time: 20–30 min. Monomer composition: 73/27 ABA/ANA. Reaction temperature: 230 °C.

micrographs of a 73/27 ABA/ANA polymerization system with a reactant thickness of $\sim 10 \mu\text{m}$. These micrographs are taken from the same area of the same sample and illustrate the whole process of morphological changes at 230 °C. At the evaluated temperature, the reaction system becomes a homogeneous phase after the monomers melt (Figure 2a). During the polymerization reaction, the liquid crystal phase forms and separates from the isotropic phase once the chain length of the oligomers reaches a critical value, as shown in Figure 2b. The dark area is an isotropic phase, while the bright areas represent the LC phase. After the appearance of LC domains, their sizes increase with reaction time, and later, the entire viewing area becomes a LC phase, as shown in Figure 2g. In the late stage of the polycondensation reaction, the volume of the reacting system decreases and causes the appearance of banded textures, as shown in Figure 2h.^{20,21} However, for the banded texture to form, there must be an air gap between glass slides. If the reaction system is sandwiched between two glass slides directly, the banded texture cannot form.

3.2. Effects of Electric Fields on the LCP Polymerization System. One important complication when incorporating electric fields into organic LC materials is electrode effects because LCs usually are weak electrolytes.¹ To identify the electrode effects, we carried out the experiments by inserting a very thin insulating

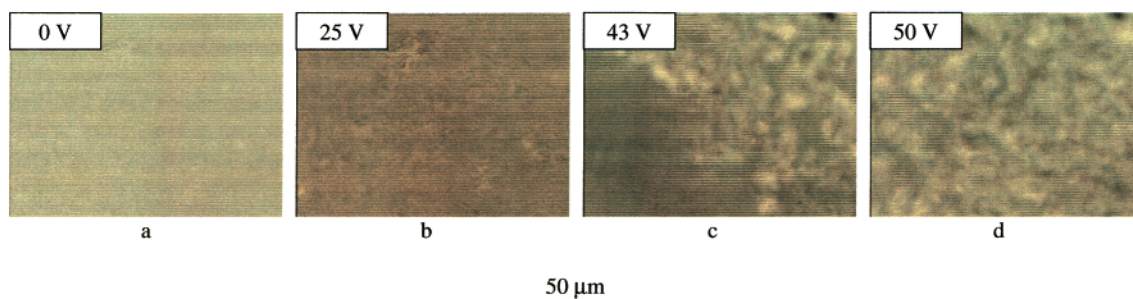


Figure 5. Morphologies of the LC phase under ac electric fields with 10 Hz frequency and different voltages: (a) 0, (b) 25, (c) 43, and (d) 50 V. Range of reaction time: 20–30 min. Monomer composition: 73/27 ABA/ANA. Reaction temperature: 230 °C.

PTFE film (20 μm) between one of the conductive glass slides and the polymerization system, and we sandwiched the reaction system directly between two conductive glass slides with full contact. For both systems, those insulated by a PTFE film and those without a PTFE film, the electrohydrodynamic instability of the LC phase can be clearly observed in relatively wide ranges of frequency and voltage. The similar results of these two different methods indicate that the electrode effects in our experiments do not play an important role. To present clearer microscope pictures, we obtained the results in this paper by the direct contacting method without PTFE films.

3.2.1. Appearance of the LC Phase on the Conductive Glass Surface. In our experiments, the electric field is applied on the polymerization system after the whole viewing area becomes a LC phase. Figure 3 shows the appearance of the LC phase before the application of the electric field. Unlike the reaction on a normal glass slide, the LC phase generated on the conductive coating layer tends to form big separated LC droplets instead of the uniform LC thin layer. This phenomenon is not because of the thickness difference in different systems but because of the difference in surface properties between the normal glass slide and the ITO-coated conductive layer. From panels c–g of Figure 3, the bigger LC domains can be seen to attract the smaller LC domains to increase their areas. Finally, a large LC domain forms and occupies the whole viewing area, as shown in Figure 3h.

Since we have to use a relatively thick sample (80 μm) in observing the electrohydrodynamic instability, the morphological change in the thick sample is slower than the one discussed in section 3.1. This is due to the fact that it is more difficult for acetic acid to diffuse out from a thicker sample, and thus, the reaction is slower.

3.2.2. Responses of the LC Phase under Electric Fields with Different Frequencies and Voltages. During the polymerization and after the whole viewing area becomes a LC phase, we apply ac electric fields with different frequencies and voltages on the reaction system to observe the effects of electric fields on the LC phase. The electric responses reported in this section are for the reaction time ranging from 20 to 30 min.

Figure 4 shows the morphologies of the LC phase at different voltages when the frequency is 1 Hz. At this low frequency, the molecular orientation can be found in the low-voltage region. To precisely detect the changes under the electric fields, we chose an area without defects and with uniform orientation for our study. Figure 4a shows the LC phase without an electric field in this area. Figure 4b depicts the pictures of the LC phase after the application of an external field of 25 V (root-mean-square). Because of the periodical oscillation of the electric field direction, the morphology exhibits periodical change; two pictures were therefore snapped with time intervals of 0.5 s. Under the electric field, the LC phase becomes more transparent

and twinkles when the electric field changes its direction. Figure 4c illustrates that electrohydrodynamic instability is observed in the high-voltage region. When the voltage is 50 V, two kinds of textures appear alternatively when the external field changes its direction. With further increase in the voltage (Figure 4d), some dark dots as vortex centers appear, and the eddy flows of LC materials can be clearly observed around the vortex centers.¹²

Figure 5 exhibits the morphologies of the reaction system under 10 Hz electric fields with different voltages. In the low-voltage range, similar orientation can be observed when comparing the LC morphologies with and without external fields in panels a and b of Figure 5. The major differences between the responses under 1 and 10 Hz fields are that the LC phase under a 10 Hz field does not flicker obviously and shows signs of electrohydrodynamic instability at a lower applied voltage. For example, Figure 5 indicates that the flow of the LC phase can be noticed in some areas when the voltage reaches 43 V. The electrohydrodynamic instability extends to the entire viewing area and becomes more violent when a higher voltage is applied. This kind of turbulent flow indicates that the system enters the dynamic scattering region.^{1,2,12}

With an increase in frequency, electrohydrodynamic instability can be found in a relatively wide range of voltage, while the effect of external fields on orientation becomes less visible. When the applied voltage is 25 V, the electrohydrodynamic flow begins to form once the frequency reaches 100 Hz. The frequency of 100 Hz is regarded as the low boundary of the electrohydrodynamic flow region under the 25 V field. This kind of flow occurs in a wide range of frequencies, from 100 Hz to 60 kHz, as shown in Figure 6. Under the same voltage, the flow seems to be faster in the middle-frequency region. The flow patterns for 10 and 50 kHz (panels c and d, respectively, of Figure 6) are quite similar to the fluctuating Williams domains which have been reported for other polymeric nematic LCs.^{11,12} The flow becomes faster if the applied voltage is increased. However, our experiments indicate that there is no distinct morphological change from the fluctuating Williams domains to the dynamic scattering mode for the polymerized LCP system. The major difference between them is the rate of flow, which is faster for the dynamic scattering mode.

When the frequency is further increased, the effect of the electric fields on the LC phase becomes undetectable because the director of the LC cannot follow the field and exhibits an almost stationary distribution. The frequency for the system entering the stationary state is regarded as the high boundary of the electrohydrodynamic flow region. When voltages are 25, 50, and 80 V, the corresponding high boundaries are 60, 75, and 85 kHz, respectively. The higher the applied voltage, the greater the critical frequency. Figure 7 is an extension of Figure 6, showing some examples of stationary LC morphologies under high-frequency fields where the voltage is 25 V. When these

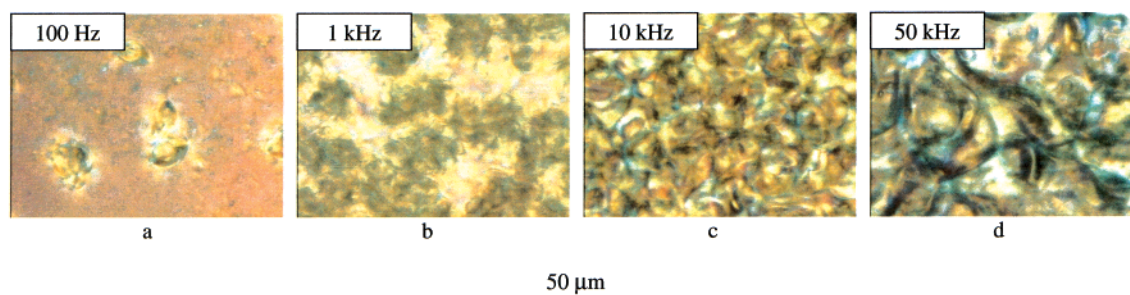


Figure 6. Morphologies of the LC phase under ac electric fields with 25 V voltage and different frequencies: (a) 100 Hz, (b) 1 kHz, (c) 10 kHz, and (d) 50 kHz. Range of reaction time: 20–30 min. Monomer composition: 73/27 ABA/ANA. Reaction temperature: 230 °C.

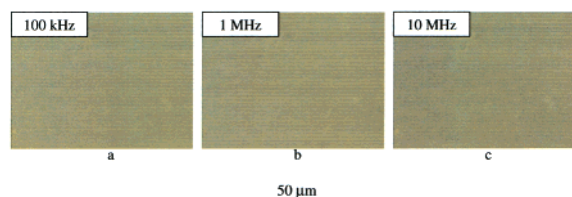


Figure 7. Morphologies of the LC phase under ac electric fields with 25 V voltage and different frequencies: (a) 100 kHz, (b) 1 MHz, and (c) 10 MHz. Range of reaction time: 20–30 min. Monomer composition: 73/27 ABA/ANA. Reaction temperature: 230 °C.

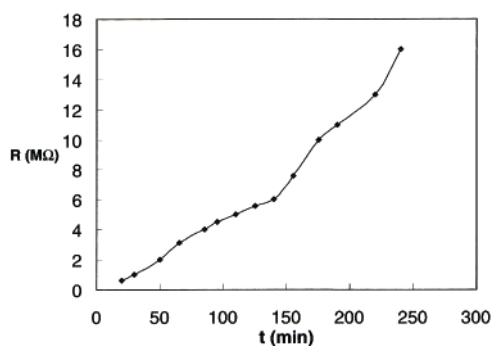


Figure 8. Dependence of the electric resistance of the reaction system on reaction time. Monomer composition: 73/27 ABA/ANA. Reaction temperature: 230 °C.

pictures are compared with those without an electric field (Figure 4a), no distinct difference can be found.

3.3. Evolution of the LC Phase during Polymerization under Electric Fields. During the polycondensation reaction, the physical properties of the LC phase vary with time.^{20–22} Both the viscosity of the reaction system and the elastic constants of LC molecules increase, while the conductivity decreases with increasing molecular weight. The changes in these parameters strongly influence the electric responses of the reaction system under external fields.

Figure 8 shows the dependence of the electric resistance of the polycondensation reaction system on reaction time. In the early stage of polymerization, the molecular weight of oligomers is low; thus, the electric resistance of the reaction system is relatively low. The resistance continuously increases with increasing reaction time, indicating that the degree of polymerization increases.

The changes of inherent properties during polymerization cause the changes in electric responses of the LC phase under external fields. Figure 9 compares the LC phase morphologies at different reaction times under the electric field with a frequency of 1 Hz and a voltage of 25 V. After a reaction time of 40 min, the orientation can still be observed through the flickering of the LC phase (Figure 9a). However, the difference

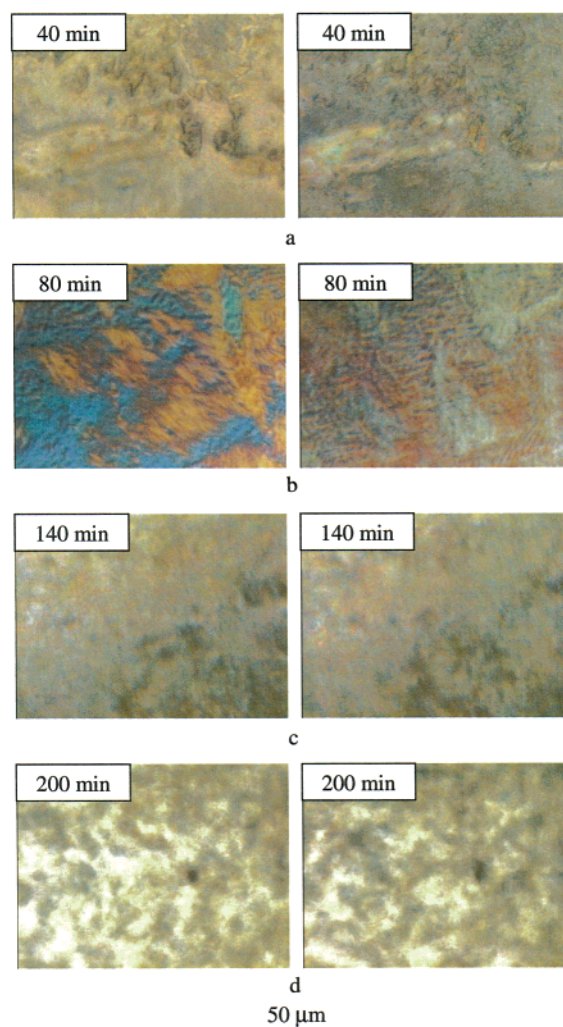


Figure 9. Comparison of the morphologies of the LC phase under electric fields with a frequency of 1 Hz and a voltage of 25 V at different reaction times: (a) 40, (b) 80, (c) 140, and (d) 200 min. Monomer composition: 73/27 ABA/ANA. Reaction temperature: 230 °C.

between the bright and dark states is not as obvious as that with reaction times from 20 to 30 min (Figure 4b). After 80 min of reaction, the LC phase forms the texture shown in Figure 9b. When the two pictures snapped with a time interval of 0.5 s are compared, two states are found to exist: one is brighter, and the other is darker. When the reaction time reaches 140 min, the situation changes, and an electrohydrodynamic flow begins to form, accompanied by a kind of to-and-fro movement (Figure 9c). This phenomenon is mainly caused by an increase in viscosity in the reaction system. If the viscosity is too low, this movement cannot be observed because the LC domain

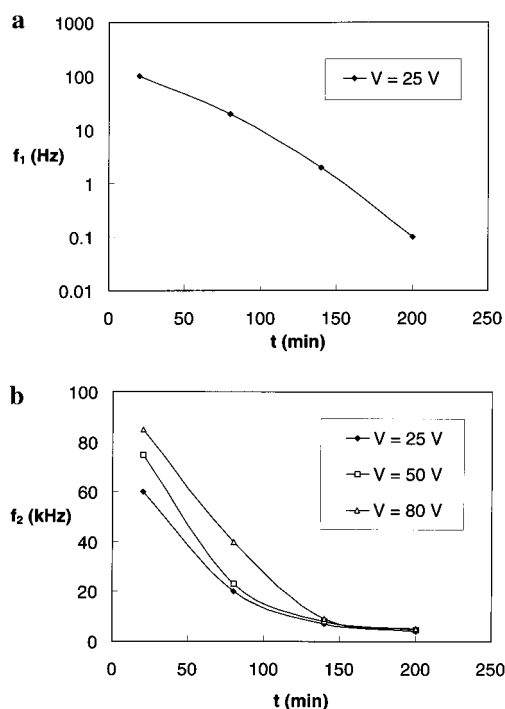


Figure 10. Low bound f_1 (a) and the high bound f_2 (b) of the electrohydrodynamic flow regime at different reaction time levels. Monomer composition: 73/27 ABA/ANA. Reaction temperature: 230 °C.

director can be easily and quickly oriented. After 200 min of reaction, the electrohydrodynamic flow becomes more obvious (Figure 9d). When the reaction time reaches 240 min, no detectable excitation can be noticed after the application of the electric field because of the high viscosity and extremely slow movement. The change of LC-phase responses during the polymerization under 10 Hz is similar to that under 1 Hz. In short, the orientation state changes to the electrohydrodynamic flow state.

At medium frequencies (60–100 kHz), the response change of the LC phase under the external field is simpler than that at low frequencies (1–10 Hz) during the reaction under 25 V field. This is due to the fact that the electrohydrodynamic flow already

appears in the early stage. With increasing reaction time, the turbulent flow under the same field becomes slower and slower, until finally it becomes stationary because of the increases in viscosity and electric resistance.

As discussed previously, electrohydrodynamic flow takes place at a certain frequency region under a specific voltage. For example, when the reaction time is in the range of 20–30 min and the voltage of the external field is 25 V, the frequency regime for LC movement is from 60 to 100 kHz. Therefore, two parameters, f_1 and f_2 , are chosen to describe the low- and high-frequency boundaries for forming flow patterns. Figure 10a shows the critical frequency of the low bound f_1 as a function of reaction time when the voltage is 25 V, and Figure 10b illustrates the high bound f_2 as a function of reaction time when the voltages are 25, 50, and 80 V. Since flow patterns or dynamic scattering can be observed under high-voltage fields (50 and 80 V), the low bound f_1 cannot be well-defined at these two voltages for Figure 10a. Because of the changes in conductivity and viscosity, both the low bound and the high bound decrease with increasing reaction time, as shown in Figure 10. The decrease in critical frequencies with decreasing conductivity is in agreement with the previous study.¹¹

The effect of the viscosity increase during the polycondensation reaction on the dynamics of response can be quantified by the morphological change during an electric “turn-on” process since the time for pattern formation increases with increasing viscosity² (for examples, see Figure 11). The incubation times are varied to yield the similar morphologies during a “switch-on” process if the reaction times are different. It takes 30 s to fully develop a flow pattern when the reaction time is around 140 min, while it takes a much longer time, 120 s, to develop a similar flow pattern when the reaction time reaches 200 min.

3.4. FTIR Characterization. Figure 12 shows the FTIR spectra of monomers and polymers. Figure 12a is the spectrum of a 73/27 ABA/ANA monomer mixture. The band at 1685 cm^{-1} is the $\nu_{\text{C=O}}$ of the $-\text{COOH}$ group, and the band at 1759 cm^{-1} is the $\nu_{\text{C=O}}$ of the $\text{CH}_3\text{COO}-$ group. By monitoring the change in acetoxy and carboxyl groups with FTIR, we can obtain insights into the thin-film polymerization reaction. After 5 h of reaction, as shown in Figure 12b, the bands at 1685 and 1759 cm^{-1} almost completely disappear, which indicates that

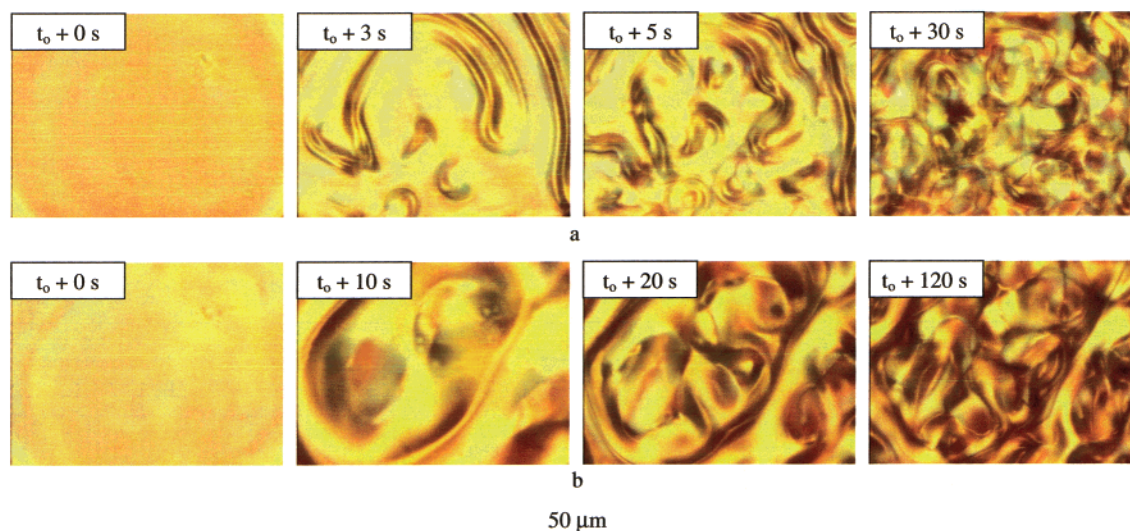


Figure 11. Comparison of the morphologies of the LC phase during electric “turn-on” processes at different reaction time levels: (a) 140 and (b) 200 min. The frequency of the ac electric field is 1 Hz. The voltage of the ac electric field is 25 V. t_0 is the time of switching on the electric field. Monomer composition: 73/27 ABA/ANA. Reaction temperature: 230 °C.

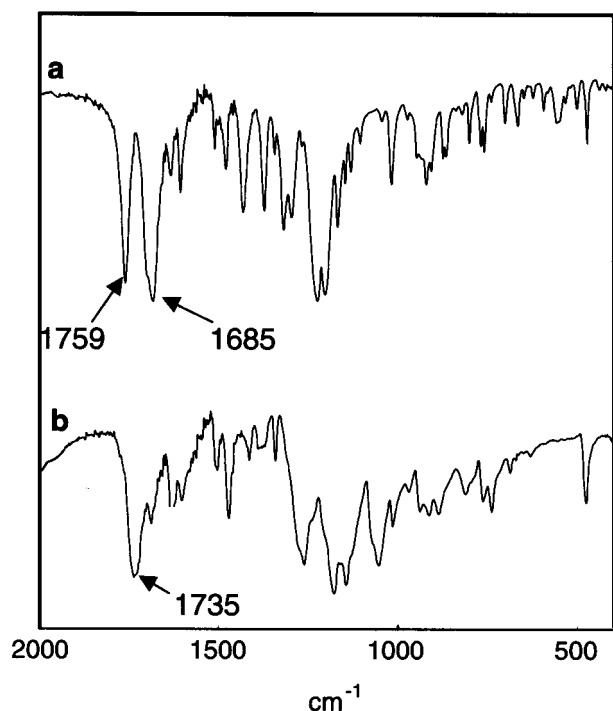


Figure 12. FTIR spectra of the monomer mixture and the thin-film polymerization product. (a) Monomer mixture: 73/27 ABA/ANA. (b) Product of a 5 h reaction at 230 °C.

nearly all the acetoxy and carboxyl groups are consumed, with a substantial number of ester groups formed at 1735 cm^{-1} , implying that the polymer is obtained.²¹

4. Conclusions

Through in situ observation during the polymerization reaction of a thermotropic main-chain LCP under ac electric fields using a polarizing microscope, we studied the effects of external fields on the dynamic response of LC phases in detail. After the appearance of the LC phase, electric fields with different voltages and different frequencies were applied to the polymerization system. The frequency and the strength of an external field determine the dynamic response and LC morphology. In the low-frequency region, a low voltage tends to induce molecular orientation, while a high voltage results in dynamic scattering. In the medium-frequency region, electrohydrodynamic flow can be clearly observed. With further increasing frequency, no visible change is found in a relatively large voltage range because the molecular director in the LCP phase cannot

respond so fast. Because of the continuous changes in viscosity, elastic constants, and conductivity during the polycondensation reaction, the electric response of the LC phase changes with the reaction time accordingly. Under a certain voltage, the low and high bounds of electrohydrodynamic flow regime decrease with increasing reaction time.

Acknowledgment. The authors thank the National University of Singapore (NUS) for the research fund, the Institute of Materials Research and Engineering (IMRE) for the equipment. Special thanks are due to Dr. S. Mullick for providing the monomers and Dr. Y. H. Lin, Dr. C. B. He, and Mdm. L. K. Leong for their kind help.

References and Notes

- (1) de Gennes, P. G.; Prost, J. *The Physics of Liquid Crystal*; Clarendon Press: New York, 1993.
- (2) Blinov, L. M.; Chigrinov, V. G. *Electrooptic Effects in Liquid Crystal Materials*; Springer-Verlag: New York, 1994.
- (3) Kelker, H.; Hatz, R. *Handbook of Liquid Crystals*; Verlag Chemie: Weinheim, Germany, 1980.
- (4) Hidaka, Y.; Huh, J. H.; Hayashi, K.; Kai, S. *Phys. Rev. E* **1997**, 56, R6256.
- (5) Toth, P.; Buka, A.; Peinke, J.; Kramer, L. *Phys. Rev. E* **1998**, 58, 1983.
- (6) John, T.; Stannarius, R.; Behn, U. *Phys. Rev. Lett.* **1999**, 83, 749.
- (7) Medya, R. K.; Choudhary, R. N. P.; Mahapatra, P. K. *Liq. Cryst.* **1999**, 26, 795.
- (8) Lucchetta, D. E.; Scaramuzza, N.; Strangi, G.; Versace, C. *Phys. Rev. E* **1999**, 60, 610.
- (9) Shehadeh, H. M.; McClymer, J. P. *Phys. Rev. Lett.* **1997**, 79, 4206.
- (10) Strangi, G.; Versace, C.; Scaramuzza, N.; Lucchetta, D. E.; Carbone, V.; Bartolino, R. *Phys. Rev. E* **1999**, 59, 5523.
- (11) Krigbaum, W. R.; Grantham, C. E.; Toriumi, H. *Macromolecules* **1982**, 15, 592.
- (12) Krigbaum, W. R.; Lader, H. J.; Ciferri, A. *Macromolecules* **1980**, 13, 554.
- (13) Tanaka, K.; Takahashi, A.; Akiyama, R.; Kuramoto, N. *Phys. Rev. E* **1999**, 59, 5693.
- (14) Körner, H.; Shiota, A.; Bunning, T. J.; Ober, C. K. *Science* **1996**, 272, 252.
- (15) Donald, A. M.; Windle, A. H. *Liquid Crystalline Polymers*; Cambridge University Press: Cambridge, 1992.
- (16) Shibaev, V. P.; Lam, L. *Liquid Crystalline and Mesomorphic Polymers*; Springer-Verlag: New York, 1994.
- (17) Chung, T. S.; Calundann, G. W.; East, A. J. *Encycl. Eng. Mater.* **1989**, 2, 625.
- (18) Chung, T. S. *Polym. Eng. Sci.* **1986**, 26, 901.
- (19) Liu, J.; Rybníkar, F.; Geil, P. H. *J. Macromol. Sci., Phys.* **1996**, B35, 375.
- (20) Cheng, S. X.; Chung, T. S.; Mullick, S. *Chem. Eng. Sci.* **1999**, 54, 663.
- (21) Cheng, S. X.; Chung, T. S. *J. Phys. Chem. B* **1999**, 103, 4923.
- (22) Cheng, S. X.; Chung, T. S.; Mullick, S. *J. Polym. Sci. Phys. B* **1999**, 37, 3084.
- (23) Chung, T. S.; Cheng, S. X. *J. Polym. Sci. Chem. A* **2000**, 38, 1257.
- (24) Cheng, S. X.; Chung, T. S. *J. Polym. Sci. Phys. B* **2000**, 38, 2221.